Performance Analysis of Beta-Type Stirling Cycle Refrigerator for Different Working Fluids

Muluken Z. Getie[1,2,3(✉)], Francois Lanzetta[1], Sylvie Begot[1], Bimrew T. Admassu[3], and Steve Djetel Gothe[1]

[1] FEMTO-ST Institute, Univ. Bourgogne Franche-Comte, CNRS Parc technologique, 2 avenue Jean Moulin, F-90000 Belfort, France
muluken.zegeye@bdu.edu.et

[2] Bahir Dar Energy Center, Bahir Dar Institute of Technology, Bahir Dar University, Bahirdar, Ethiopia

[3] Faculty of Mechanical and Industrial Engineering, Bahir Dar Institute of Technology, Bahir Dar University, Bahirdar, Ethiopia

Abstract. The Stirling cycle refrigerators, which are the counterparts of the Stirling engines are of gas cycle machines. In the present paper, experimental investigation and numerical analysis of Beta-type Stirling refrigerator for domestic applications are conducted. The refrigeration performances such as input power requirement, cooling power, and coefficient of performance for moderate temperature applications have been analyzed using different working fluids (air, nitrogen, helium, and hydrogen). The numerical analysis is conducted to evaluate the performance of a machine with respect to different operating frequencies and charging pressures. The result of the analysis showed that air and nitrogen have better cooling power than helium and hydrogen in the operating ranges (15–25 bar and 6–12 Hz) of the cooling machine. On the other hand, the coefficient of performances in the case of helium shows a higher rate of increase with charging pressure than that of air and nitrogen.

Keywords: Beta type · Experiment · Moderate cooling · Different working fluid · Cooling power

M. A. Delele et al. (Eds.): ICAST 2020, LNICST 385, pp. 286–301, 2021.
https://doi.org/10.1007/978-3-030-80618-7_19

Nomenclature

A= cross sectional area (m^2)
C_p= isobaric specific heat ($J.kg^{-1}.K^{-1}$)
C_v= isochoric specific heat ($J.kg^{-1}.K^{-1}$)
K = heat conductivity ($W.m^{-1}.K^{-1}$)
L =length (m)
M = mass of working gas (kg)
$\dot{m}$ = mass flow rate ($kg.s^{-1}$)
P = pressure (Pa)
Q = heat (J)
R = gas constant ($J.kg^{-1}.K^{-1}$)
T = temperature (^oC)
V = volume (m^3)
V_d= instantaneous swept volume of displacer (m^3)
V_{swc}= swept volume of compression (m^3)
W = work (J)

Greek symbols

ε = regenerator effectiveness
η = clearance effciency
γ = ratio of specific heats (C_p /C_v)
θ = crank angle (^{o})
ω = omera ($rad.s^{-1}$)

subscripts

c = compression space
cr = chiller
e = expansion space
g= gas
h = hot heat exchanger
leak = leakage
mean = mean value
r = regenerator
shut = shuttle
t = total

1 Introduction

Recently, due to the limitation of fossil fuels and their environmental impact, researchers in the area of motor have been forced to explore other types of machines that could substitute fossil fuel-driven engines. Stirling cycle engine is one of the alternatives as it runs with environmentally friendly gases. Stirling cycle machine is a type of external heat engine with a closed thermodynamic cycle. Robert Stirling invented the first Stirling machine in 1816as a heat engine to produce mechanical energy from heat energy. In this Stirling engine, the working fluid used to replace the steam engines was air. By reversing the cycle, the Stirling engine can operate as a heat pump or cooling machine. The Stirling cycle engine was first realized as a cooling machine in 1832 [1]. In 1862 Alexander Kirk developed a practical Stirling cycle cooler [2]. Subsequently, different researches have been conducted on Stirling cycle cooling machines and the detailed review is presented in [3].

The configurations of Stirling cycle machines are generally grouped based on piston and piston/displacer-cylinder arrangement as the Alpha, Beta, and Gamma configurations [4–6]. Different configurations have different mechanical designs but are working with the same thermodynamic cycles. Different configurations of the Stirling refrigerator have been investigated [7–11]. The optimal relationship between the cooling power and the coefficient of performance of the Stirling cycle refrigerating machine was conducted in different researches [12–14]. A general analytical model has been introduced for various applications of the Stirling refrigerator [15].

The V-type Stirling refrigerator was thermodynamically analyzed [16–18]. The impact of working fluids on the performance of a V-type Stirling cycle refrigerating machine for a charging pressure less than 5 bar was investigated [17]. The integral V-type

Stirling refrigerator was developed, tested, and proven as a domestic cooling machine [18]. The reported COP for such machines varied between 0.1 and 0.9 under different working parameters. The performance parameters, such as the input power demand and the coefficient of performance were examined under different turning speeds and charging pressures. An isothermal model was developed for an Alpha type Stirling cryocooler by considering various losses and the effects of various parameters on cooling performance were investigated [19]. From the research, it has been reported that heat conduction loss was the biggest heat loss and loss due to mechanical friction was the biggest work loss.

Batooei A. et al. conducted the optimization of the Stirling refrigerator based on the experimental and numerical methods for Gamma configuration [20]. The numerical method applied by this research is multi-objective optimization using non-ideal adiabatic conditions. The cooling capacity and the COP were experimentally investigated for helium and air as a working fluid. The experimental and numerical results from the research proved that the production of cold increases continuously with the rotational speed whereas COP has an optimum value. Theoretical and experimental evaluation of the Gamma-type Stirling refrigerator was conducted [21]. The optimum theoretical and experimental analysis coefficients of performances from the research were reported as 0.28 and 0.27 respectively.

Oguz et al. [22] conducted an experimental work for free-piston Stirling coolers. It has been reported that the COP values for coolers operating with ambient temperatures close to 30° C were found between 2 and 3 for cold head temperatures around 0° C and decreasing to around 1 for cold temperatures near to −40° C. The effect of parameters such as dead volume ratio, compression ratio, types of working fluids, and the phase angle on the performance of a Beta-type refrigerating machine was studied [23]. A 100 W Beta-type Stirling cycle refrigerator was designed and experimentally tested [24]. A thermodynamic model was developed and an experimental validation was conducted for optimizing Beta-type Stirling refrigeration machines using air as a working fluid [25]. Evaluation of the effect of geometrical parameters such as dead space volume and swept volume on the performance of the refrigerating machine was the special emphasis for this research. A Beta-type Stirling cooler was developed with a rhombic drive system [26]. In the same year, a similar configuration Stirling refrigerator was designed and fabricated to achieve a rapid transfer of heat from the system [27]. Helium and carbon dioxide have been used as a working fluid and the more efficient fluid was determined.

Generally, Stirling cycle machines are characterized by high thermal efficiency, low emissions, low vibration, low noise, the ability to use almost all types of thermal energy source, safe operation, low maintenance, and reversible working cycle. Furthermore, the findings of most researches done so far proved that Stirling cycle machines are promising alternatives for moderate temperature cooling applications. On the other hand, a limited number of researches have been conducted on these types of Stirling cycle refrigerators. Therefore, more studies are needed to enhance the performance of Stirling refrigerators in this application. In the present study, the developed numerical model is validated using an experiment and the effect of working fluid on the refrigerating performance is analyzed for moderate cooling applications. The analysis is conducted for air, nitrogen, helium, and hydrogen at different operating frequencies and charging pressure.

2 Mathematical Modeling

2.1 Adiabatic Modeling

The Stirling cycle machine consists of two variable volumes (compression and expansion) spaces physically separated by a regenerator and at different temperatures. For the Stirling cycle refrigerator, heat is absorbed from the low temperature heat source, and heat is stored and released in the regenerator (see Fig. 1). An ideal Stirling cycle refrigerator consists of four separate thermodynamics processes, which consists of two isothermal processes and two constant volume processes as shown in Fig. 2.

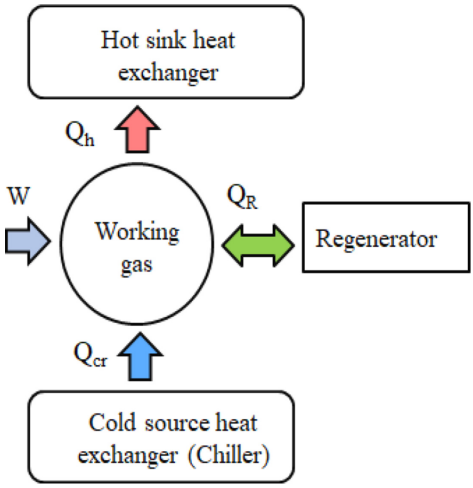

Fig. 1. Schematic diagram of Stirling refrigerator

In real Stirling cycle machines, the compression and expansion processes tend to be adiabatic. Therefore, the basis of this work is an ideal adiabatic analysis. For easy of analysis, the overall Stirling refrigeration machine is configured into five control volumes (two working spaces and three perfectly effective heat exchangers) serially connected, the model is similar to Urieli and Berchowitz model [6]. The governing equations of the adiabatic equation are shown in Table 1.

The ideal adiabatic equation is modified by incorporating shuttle heat loss and gas leakage to the crankcase. This is because these losses have a direct impact on working conditions (pressure and temperature) of working fluid and hence on the overall performance of the machine. So, differential equations of mass and energy conversations of the original ideal adiabatic analysis of the Stirling refrigeration machine have been modified including the effect of mass leakage and shuttle heat losses.

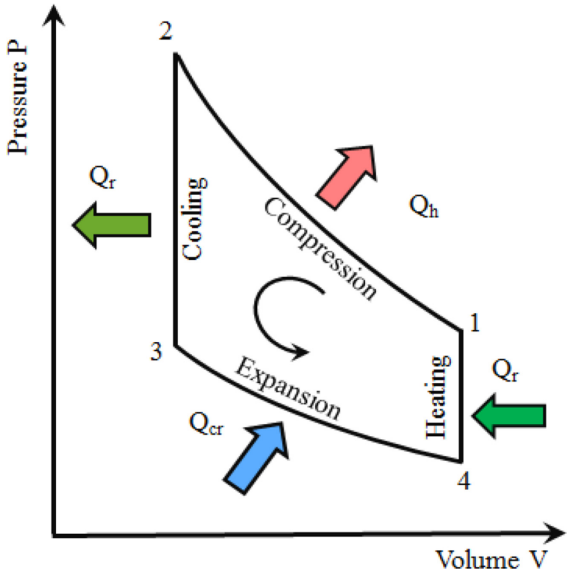

Fig. 2. PV- diagram of an ideal Stirling cycle refrigerator

Table 1. Governing equations of ideal adiabatic analysis (adapted from [6])

Equation set	Parameters
$\mathrm{DP} = \frac{-\gamma \mathrm{P}\left(\frac{DVc}{Tch} + \frac{DVe}{Tcre}\right)}{\left[\frac{Vc}{TCh} + \gamma\left(\frac{Vh}{Th} + \frac{Vr}{Tr} + \frac{Vcr}{TCr}\right) + \frac{Ve}{Tcre}\right]}$	Pressure changes in the system
$\mathrm{Dm} = \left(\frac{\mathrm{pDV} + \mathrm{VDp}/\gamma}{\mathrm{RT}}\right)$	Mass accumulation
$\mathrm{DT} = \mathrm{T}\left(\frac{\mathrm{DP}}{\mathrm{P}} + \frac{\mathrm{DV}}{\mathrm{V}} - \frac{\mathrm{Dm}}{\mathrm{m}}\right)$	Temperature change
$DQ = \frac{VC_v DP}{R} - C_p\ (T_{in}\dot{m}_{in} - T_{out}\dot{m}_{out})$	Heat power in three heat exchangers
$D\ \mathrm{W} = \mathrm{PDV}$	power

The details of the analysis are presented in [28]. The final equations affected by the mass leakage and shuttle heat loss are presented in Eqs. (1, 2, and 3). The other equations remain unchanged as of the ideal adiabatic model.

$$DP = \frac{-\gamma P\left(\frac{DV_c}{Tch} + \frac{DV_e}{Tcre}\right) + \gamma R \frac{\mathrm{DQ_{shut}}}{\mathrm{C_p}}\left(\frac{T_{ch} - T_{cre}}{T_{ch}T_{cre}}\right) + \gamma R D m_{leak}}{\left[\frac{V_c}{TCh} + \gamma\left(\frac{Vh}{Th} + \frac{Vr}{Tr} + \frac{Vcr}{TCr}\right) + \frac{V_e}{Tcre}\right]} \tag{1}$$

$$Dm_c = \left(\frac{PDV_c + V_c Dp/\gamma}{RT_{ch}}\right) + \frac{DQ_{shut}}{C_p T_{ch}} \tag{2}$$

$$Dm_e = \left(\frac{pDV_e + V_eDp/\gamma}{RT_{cre}}\right) - \frac{DQ_{shut}}{C_pT_{ch}} \tag{3}$$

2.2 Modified Simple Analysis

The heat and power losses that do not have direct impact on the operating condition of a Stirling cycle machine are separately analyzed. These thermal and power losses are assumed as independent to each other and the total losses are the summation of the losses with the respective category. The losses incorporated in modified simple analysis are summarized in Table 2 as developed by the researchers' previous work [28].

Table 2. Summary of losses included in modified simple analysis [28]

No	Types of losses	Equations
1	Heat losses due to internal conduction in the regenerator	$Q_{wrl} = k\frac{A}{L}(Twh - Twcr)$
2	Loss due to regenerator ineffectiveness/external conduction	$Q_{rl} = \dot{m}c_p(1-\varepsilon)(T_c - T_e)$
3	Loss due to pressure drop in heat exchangers	$W_{fr} = \int_0^{2\pi}(\Delta P\frac{dV_e}{d\theta})d\theta$, $\Delta P = \Delta p_h + \Delta p_r + \Delta p_{cr}$
4	Heat conduction loss	$Q_{cond} = k\frac{A}{L}\Delta T$
5	Pumping loss	$\dot{Q_p} = (1-\eta)\dot{m}C_p(T_c - T_e)$
6	Loss due to finite speed of piston	$W_{fin-sp} = 2\Delta p_{fin.sp}.V_{swc}$
7	Mechanical Friction loss	$W_{mec.fr} = 2\Delta p_{mec.fr}.V_{swc}$
8	Gas Spring hysteresis loss	$W_{gs} = \sqrt{\frac{1}{32}\omega\gamma^3(\gamma-1)T_wP_{mean}Kg}(V_d/2V_t)^2A_w$

3 Experimental Setup

The considered experimental machine is a reversible thermal machine (motor and/or receiver) with Beta configuration and operates between two constant temperatures. This machine consists of expansion space, heater (acts as a chiller in case of the cooling machine), regenerator, cooler (acts as a hot heat exchanger in case of the cooling machine), compression space, piston, buffer space, and driving mechanisms. The power piston and displacer are arranged within a single cylinder. The displacer piston controls the variations of the expansion volume (cold room) and the power piston controls the compression space (hot room) for such Stirling refrigerating machine. The setup includes a regenerative Stirling refrigerator, cooling water system, the electric supplier, and a data

acquisition system. The refrigerator is arranged with six thermometers and one pressure sensor for measuring the working conditions. The setup of the refrigerating machine is demonstrated in Fig. 3.

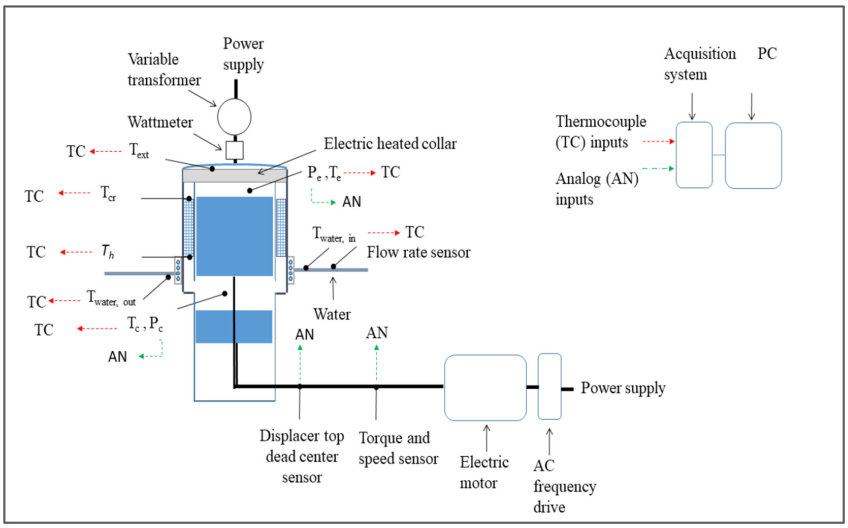

Fig. 3. Experimental setup of Stirling refrigerator

The hot heat exchanger and the chiller both have slot geometric arrangement and the configuration of the regenerator is an annular configuration with a stainless-steel woven screens' matrix. The main parameters and dimensions of the experimental device are shown in Table 3.

Table 3. Experimental engine specification

No	Parameters	Value
1	Hot heat temperature (°C)	32
2	Cooling temperature (°C)	−5
3	Piston diameter (mm)	60
4	Displacer diameter (mm)	59
5	Piston stroke (mm)	40
6	Compression space swept volume (cm^3)	103
7	Expansion space swept volume (cm^3)	113
8	Working gas	Nitrogen
9	Frequency (Hz)	7.5
10	Charging pressure (bar)	20

The refrigeration rotational speed varied between 435 to 725 rpm and the charging pressure is varied between 15–25 bar. The cooling capacity, coefficient of performance of the refrigerating machine, and minimum achievable no-load temperature of a Stirling refrigerator are determined experimentally. The thermal load was applied by two resistance heaters to the cold head of the Stirling cycle refrigerator, and steady-state characteristics of the refrigerator were measured. For a varied input voltage, different tests were carried out to determine the variation of the cooling performance with the cold head temperature of the coolers varied from −40 °C to 0 °C. The detailed experimental setup is presented in [28, 29]. The working gas considered in the experiment is nitrogen, which is assumed to behave like a perfect gas.

Table 4. Experimental results at a charging pressure of 17.5 bar (Nitrogen)

Parameters	Experiment 1	Experiment 2	Experiment 3
Electric power (W)	1650	1640	1460
Power loss electrical (W)	285.2	280.5	251
Power mechanical (W)	1365	1359	1209
Cold production (W)	451	554	676
Hot water power (W)	1429	1472	1476
Cooling temperature ($^{\circ}$C)	−15.1	−4.3	10.5
Temperature at exit head ($^{\circ}$C)	−10	1	16
Speed(rpm)	721	721.8	724
Torque (Nm)	18	18	16
Mechanical COP	0.33	0.41	0.56

Table 4 illustrates the three experimental results conducted at different electrical input power. In the Table, the electrical power loss, cooling production, the temperature of a gas at the cold side, and coefficient of performance of the machine are presented. As the gas temperature at the cold end increases, both cooling production and COP increases.

Figure 4 shows a no-load temperature distribution at different parts of the refrigerating machine with Nitrogen as a working gas. Initially, the refrigerator is set at ambient temperature and once the motor is switched on, the temperature of the cold side (expansion space) drops quickly and reaches a steady-state cold-end temperature. The minimum no-load temperature is achieved at a pressure of 25 bar and a frequency of 12.1 Hz is − 68 °C. The stabilization temperature is found after 20 min of operation. It is recognized that after the machine starts running, the buffer space temperature increases considerably from around 17.4 °C to 40 °C. This confirms that there is heat loss to the buffer space.

Figure 5 is a plot of temperature variation versus time in different parts of the refrigerating machine. The experiment was run for 90 min to confirm the trend of the cooling process for a long period using nitrogen as a working gas. The stabilization temperature at the cold end is −15.1 °C at a cooling load of 451 W, charging pressure of 17.5 bar,

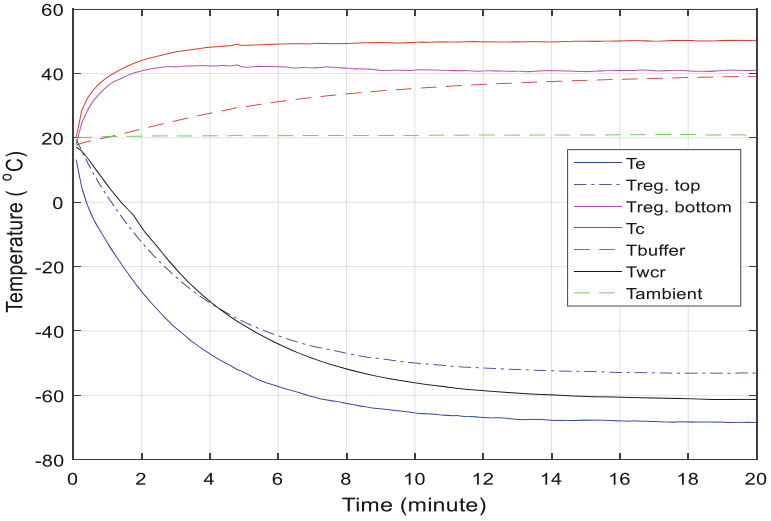

Fig. 4. No-load temperature variation at P = 25 bar and operating frequency = 12.1 Hz

and frequency of 12.1 Hz. Such Stirling refrigerator needs only 3 min to reach such a low temperature and the stabilization temperature is achieved after 40 min. The minimum temperature found is −24.9 °C and achieved 10 min after starting the operation. The buffer space temperature rises approximately by 10 °C from the ambient temperature. This result shows that there seems more gas leakage towards the buffer space that may result in heat loss. Furthermore, the stabilized temperature difference between the compression space (warm section) and the buffer space is less than 4° C.

As shown in Fig. 6, the temperature of water in the hot heat exchanger increases considerably. The heat power rejected with the flow of water at a hot heat exchanger could be given by the flow rate of water specific heat of the water and the change in temperature of water flowing in this heat exchanger.

$$\dot{Q}_h = \dot{m}_h C_p (T_{h,ex} - T_{h,in}) \tag{4}$$

Where the mass flow of water ($\dot{m}_h$) =3kg/min, specific heat of water (CP) = 4185 J.kg^{-1}K $^{-1}$, $T_{h,ex}$ is the temperature of water at the hot heat exchanger exit, and $T_{h,in}$ is the temperature of water at the entry of the hot heat exchanger.

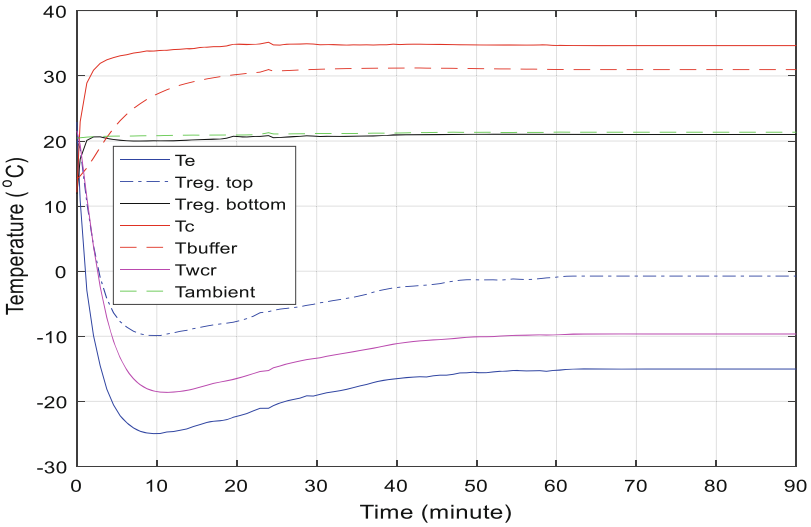

Fig. 5. Temperature distribution versus time at P = 17.5 bar, operating frequency = 12.1 Hz, and cooling load = 451 W

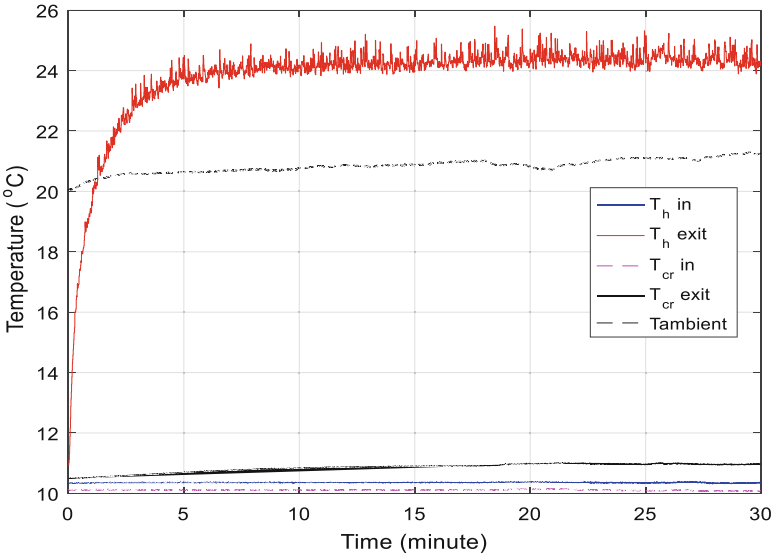

Fig. 6. The temperature of working fluid at 25 bar and 12.1 Hz

4 Results and Discussion

The numerical model is validated experimentally using the FEMTO 60 Stirling machine as described in the researchers' previous work [28]. In this part of the research, the simulation results of the analysis present the effect of different working fluids (air,

helium, hydrogen, and nitrogen). The simulation was conducted using these fluids at the different operating frequencies and charging pressures to investigate the cooling performance of the machine.

Figure 7 illustrates the required input power versus operating frequency for different working fluids (air, nitrogen, helium, and hydrogen) at $T_h = 27$ °C, $T_{cr} = -3$ °C, and a charging pressure of 17.5 bar. It can be observed that the input power requirement increases with operating frequency for all working fluids. Furthermore, it could be seen that air and nitrogen fluids require more input power than helium and hydrogen. These results confirm that air and nitrogen operate at higher flow resistance than helium and hydrogen due to a higher mass flow rate.

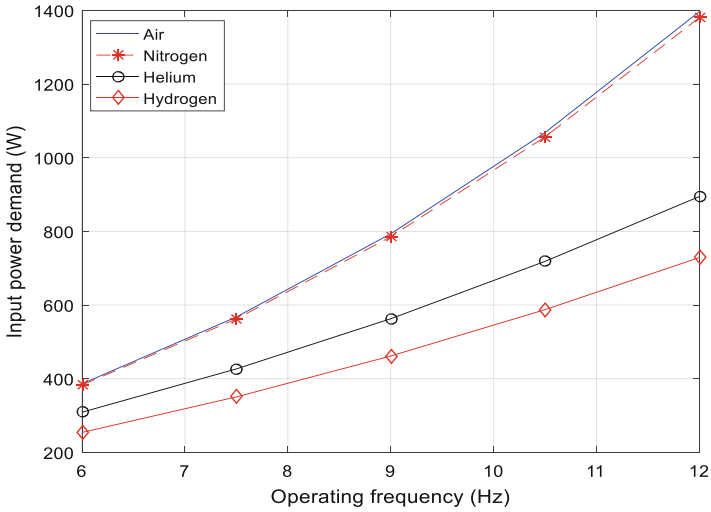

Fig. 7. Effect of working fluid on the input power requirement of with operating frequency

Figure 8 shows the impact of different working fluids on cooling power with an increase in operating frequency at $T_h = 27$ °C, $T_{cr} = -3$ °C, and a charging pressure of 17.5 bar. Similar to Fig. 7, it can be observed that the cooling power increases with the operating frequency for all working fluids types. Furthermore, it could be seen that the cooling power for air and nitrogen is higher than the cooling power of helium and hydrogen gases within the range of operating frequency 6–12 Hz. There are two potential reasons for the less cooling performance of helium and hydrogen as compared with air and nitrogen. First, the masses of helium and hydrogen are much lower than air and nitrogen, and hence a lower heat removal rate is observed and as a result lower cooling power. Second, helium and hydrogen have a higher thermal conductivity which leads to higher shuttle heat losses and these cause helium and hydrogen gases to produce lower cooling power than air and nitrogen. The shuttle heat loss has a complex effect on the cooling machine performance as it affects the working fluid pressure and temperature.

Figure 9 demonstrates the effect of different working fluids on the COP of a cooling machine with respect to operating frequency at $T_h = 27$ °C, $T_{cr} = -3$ °C, and charging

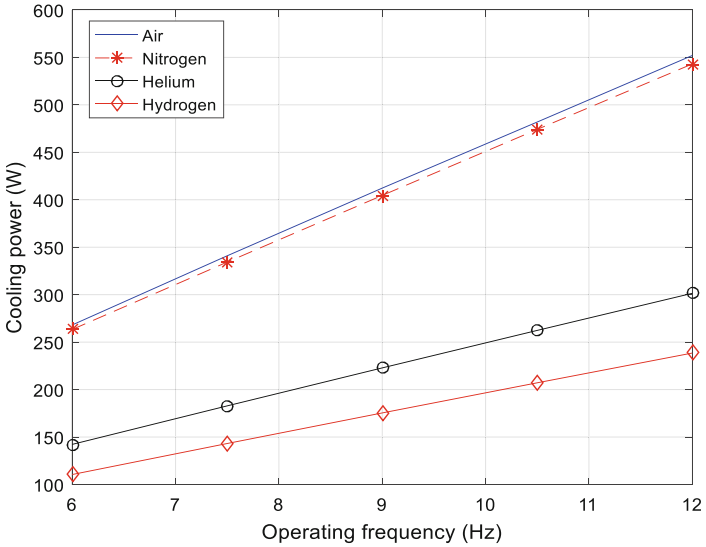

Fig. 8. Cooling capacity vs operating frequency at different working fluid types

pressure of 17.5 bar. It can be seen that air and nitrogen have better COP than helium and hydrogen within the range of operating frequency. Even though, both input power requirement and cooling power increase with operating frequency, COP decreases as a result of a higher rate of increase of flow friction and mechanical friction loss. The COP for air and nitrogen decreases radically with operating speed and this trend shows that at very high operating speed the COP for helium may be higher than the COP of air and nitrogen.

Figure 10 is a diagram demonstrating the required input power versus charging pressure for different working fluids at $T_h = 27$ °C, $T_{cr} = -3$ °C, and an operating frequency of 7.5 Hz. It can be observed that the input power requirement increases with pressure for all working fluids. Furthermore, it could be seen that air and nitrogen fluids require more input power than helium and hydrogen. This is because air and nitrogen operate at higher flow resistance than helium and hydrogen due to a higher mass flow rate for a given operating condition.

Figure 11 displays the influence of working fluids (air, nitrogen, helium, and hydrogen) on cooling power with respect to charging pressure at $T_h = 27$ °C, $T_{cr} = -3$ °C, and an operating frequency of 7.5 Hz. It can be observed that the cooling power increases with charging pressure for all working fluids. Furthermore, it could be observed that the cooling power for air and nitrogen is greater than the cooling power of helium and hydrogen due to a higher mass flow rate which leads to more heat removal rate.

Figure 12 displays the influence of working fluids on the COP of the refrigerating machine with charging pressure at $T_h = 27$ °C, $T_{cr} = -3°$ C, and an operating frequency of 7.5 bar. Air and nitrogen have by far better COP than helium and hydrogen. The COP for nitrogen increases from 53% to 73% as the charging pressure increases from 15 bar

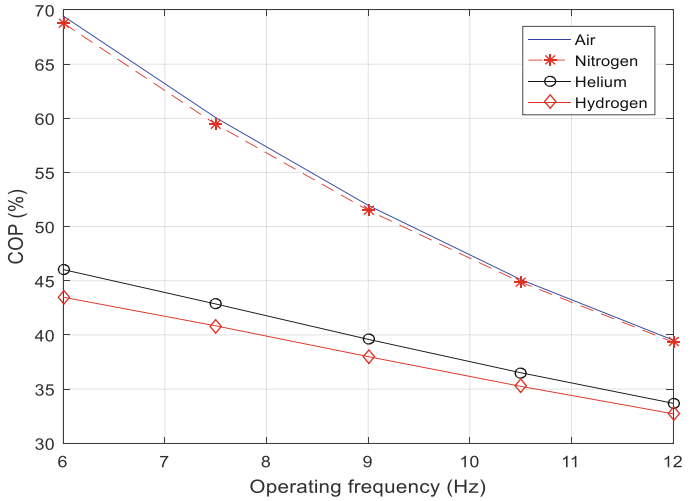

Fig. 9. COP vs operating frequency for different working fluid types

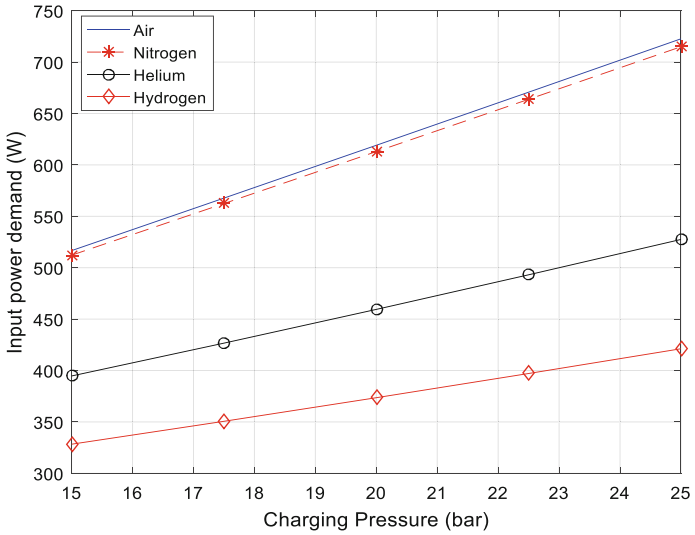

Fig. 10. Effect of different fluid types on input power requirement with pressure

to 25 bar. The COP for helium increases radically with charging pressure due to a lower rate of increase in flow friction losses as compared with air and nitrogen.

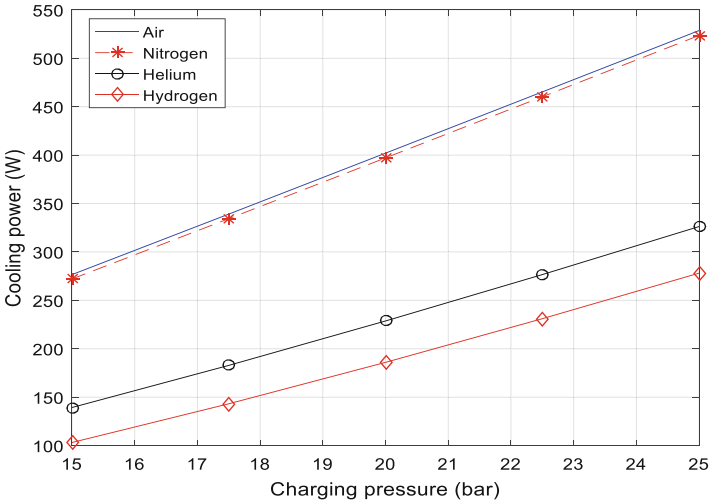

Fig. 11. Effect fluid types on cooling capacity of Stirling cycle refrigerator with pressure

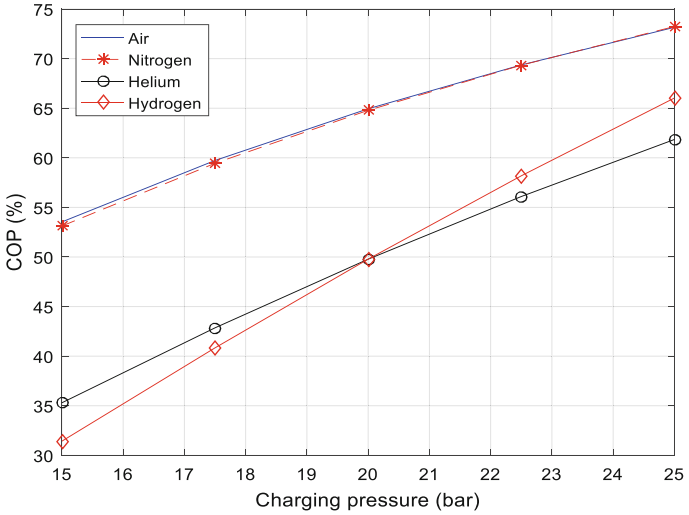

Fig. 12. COP vs charging pressure for different working fluids

5 Conclusion

In this research work, the experimental results are presented with and without load and performance analysis of the developed model is conducted for domestic cooling applications. The experimental investigation is used to determine the actual cooling power, coefficient of performance of the refrigerating machine, and minimum achievable no-load temperature of a particular Stirling cycle refrigerator. The minimum cold side no-load gas temperature was found with an experiment at a charging pressure of 25 bar

and an operating frequency of 12.1 Hz is − 68 °C. The performance of the cooling machine at different working fluids such as nitrogen, air, helium, and hydrogen are analyzed using the numerical simulation at different operating frequencies (6–12 Hz) and charging pressures (15–25 bar) of the machine within the operating range. Based on the analysis the following results have been found:

- Cooling power and input power required increased with charging pressure and with operating frequency for all considered working fluids for a typical Beta-type Stirling cycle refrigerating machine.
- COP decreases with an increase in operating frequency and increases with increasing charging pressure for all considered working fluids. The trend of COP with respect to operating frequency and charging pressure showed that helium could have better COP at higher pressure and frequency.
- Air and nitrogen have by far higher cooling power than helium and hydrogen due to more heat removal rates as a result of a higher mass flow rate.
- Air, which is an easily available gas, could be preferred as a working fluid for domestic Stirling cycle cooling machines due to better comparative performance especially in most of the operating ranges (frequency and pressure) of such machine.

Acknowledgement. This research has been supported by EIPHI Graduate School (contract ANR-17-EURE-0002) and the Region Bourgogne-Franche-Comte, by Bahir Dar institute of technology, by the Embassy of France to Ethiopia and the African Union, and by the Ministry of Science and Higher Education of Ethiopia.

References

1. Kohler, J.W.: The Stirling refrigeration cycle in cryogenic technology. Adv. Sci. **25**, 261 (1968)
2. Kirk, A. C.: On the mechanical production of cold. (includes plates and appendix). In: Minutes of the Proceedings of the Institution of Civil Engineers, vol. 37, pp. 244–282. Thomas Telford-ICE Virtual Library (1874)
3. Getie, M.Z., Lanzetta, F., Bégot, S., Admassu, B.T., Hassen, A.A.: Reversed regenerative Stirling cycle machine for refrigeration application: a review. Int. J. Refrig. **118**, 173–187 (2020)
4. Kirkley, D.: Determination of the optimum configuration for a Stirling engine. J. Mech. Eng. Sci. **4**(3), 204–212 (1962)
5. Reader, G.T., Hooper, C.: Stirling Engines. E. and F. Spon, New York, NY, USA (1983)
6. Urieli, I., Berchowitz, D.M.: Stirling Cycle Engine Analysis. A. Hilger Bristol (1984)
7. Ahmadi, M.H., Ahmadi, M.-A., Mohammadi, A.H., Mehrpooya, M., Feidt, M.: Thermodynamic optimization of Stirling heat pump based on multiple criteria. Energy Convers. Manag. **80**, 319–328 (2014)
8. De Boer, P.: Optimal performance of regenerative cryocoolers. Cryogenics **51**(2), 105–113 (2011)
9. Li, R., Grosu, L.: Parameter effect analysis for a Stirling cryocooler. Int. J. Refrig. **80**, 92–105 (2017)

10. Tyagi, S., Lin, G., Kaushik, S., Chen, J.: Thermo economic optimization of an irreversible Stirling cryogenic refrigerator cycle. Int. J. Refrig. **27**(8), 924–931 (2004)
11. Xu, Y., et al.: Operating characteristics of a single-stage Stirling cryocooler capable of providing 700 w cooling power at 77 k. Cryogenics **83**, 78–84 (2017)
12. Chen, J.: Minimum power input of irreversible Stirling refrigerator for given cooling rate. Energy Convers. Manag. **39**(12), 1255–1263 (1998)
13. Chen, J., Yan, Z.: The general performance characteristics of a Stirling refrigerator with regenerative losses. J. Phys. D Appl. Phys. **29**(4), 987 (1996)
14. Razani, A., Dodson, C., Roberts, T.: A model for exergy analysis and thermodynamic bounds of Stirling refrigerators. Cryogenics **50**(4), 231–238 (2010)
15. Ataer, Ö.E., Karabulut, H.: Thermodynamic analysis of the V-type Stirling-cycle refrigerator. Int. J. Refrig. **28**(2), 183–189 (2005). https://doi.org/10.1016/j.ijrefrig.2004.06.004
16. Guo, Y., Chao, Y., Wang, B., Wang, Y., Gan, Z.: A general model of Stirling refrigerators and its verification. Energy Convers. Manag. **188**, 54–65 (2019)
17. Tekin, Y., Ataer, O.E.: Performance of V-type Stirling-cycle refrigerator for different working fluids. Int. J. Refrig. **33**(1), 12–18 (2010)
18. Le'an, S., Yuanyang, Z., Liansheng, L., Pengcheng, S.: Performance of a prototype Stirling domestic refrigerator. Appl. Therm. Eng. **29** (2-3), 210–215 (2009)
19. Ahmed, H., Almajri, A.K., Mahmoud, S., Al-Dadah, R., Ahmad, A.: CFD modelling and parametric study of small-scale alpha type Stirling cryocooler. Energy Procedia **142**, 1668–1673 (2017)
20. Batooei, A., Keshavarz, A.: A gamma type Stirling refrigerator optimization: an experimental and analytical investigation. Int. J. Refrig. **91**, 89–100 (2018)
21. Katooli, M.H., Moghadam, R.A., Hajinezhad, A.: Simulation and experimental evaluation of Stirling refrigerator for converting electrical/mechanical energy to cold energy. Energy Convers. Manag. **184**, 83–90 (2019)
22. Oguz, E., Ozkadi, F.: An experimental study on the refrigeration capacity and thermal performance of free-piston Stirling coolers (2000)
23. Otaka, T., Ota, M., Murakami, K., Sakamoto, M.: Study of performance characteristics of a small Stirling refrigerator. Heat Transf. Asian Res. **31**(5), 344–361 (2002)
24. Gheith, R., Aloui, F., Nasrallah, S.: Experimental study of a beta Stirling thermal machine type functioning in receiver and engine modes. J. Appl. Fluid Mech. **4**, 33–42 (2011)
25. Hachem, H., Gheith, R., Aloui, F., Nasrallah, S.B.: Optimization of an air-filled beta type Stirling refrigerator. Int. J. Refrig. **76**, 296–312 (2017)
26. Cheng, C.-H., Huang, C.-Y., Yang, H.-S.: Development of a 90-k beta type Stirling cooler with rhombic drive mechanism. Int. J. Refrig. **98**, 388–398 (2019)
27. Suranjan, S., et al.: Determination of coefficient of performance of Stirling refrigeration. Int. J. Innov. Technol. Explor. Eng. (IJITEE) **8**, 2522–2529 (2019)
28. Getie, M.Z., Lanzetta, F., Bégot, S., Admmassu, B.T.: A non-ideal second order thermal model with effects of losses for simulating Beta-type Stirling refrigerating machine. Unpublished work (2021)
29. Djetel-Gothe, S., Lanzetta, F., Bégot, S., Gavignet, E.: Design, manufacturing, and testing of a Beta Stirling machine for refrigeration applications. Int. J. Refrig. **115**, 96–106 (2020)